

VIROLOGY



Virology Editorial Board

Editor-in-Chief

M. Emerman

Div. of Basic Sciences, Fred Hutchinson Cancer Research Center, 1100 Fairview Ave. North, Seattle, Washington, WA 98109-1024, USA

[Email M. Emerman](#)

Areas of expertise: HIV replication; Retroviruses; Evolution of virus-host interactions; Paleovirology



Reviews Editor

D.M. Knipe

Dept. of Microbiology and Immunobiology, Harvard Medical School, 77 Avenue Louis Pasteur, Boston, Massachusetts, MA 02115, USA

[Email D.M. Knipe](#)

Area of expertise: Herpes viruses; Viral chromatin; Virus-cell interactions; Innate immunity and viral evasion



Editors

S. Cherry

Perelman School of Medicine, Dept. of Microbiology, University of Pennsylvania, 225 Johnson Pavilion, 3610 Hamilton Walk, Philadelphia, Pennsylvania, PA 19104-6076, USA

[Email S. Cherry](#)

Areas of expertise: Arboviruses, virus-host interactions, innate immunity, genetic screens



R.C. Condit

Dept. of Mol. Genetics & Microbiology, University of Florida, 1600 S.W. Archer Street, P.O.Box 100266, Gainesville, Florida, FL 32610-0266, USA

[Email R.C. Condit](#)

Areas of expertise: Poxviruses and other cytoplasmic DNA viruses; DNA virus transcription and gene regulation; DNA Viruses of Insects



F. Goodrum

BIO5 Institute, Dept. of Immunobiology, University of Arizona, 1657 E. Helen St., Tucson, Arizona, AZ 85721, USA

[Email F. Goodrum](#)

Areas of expertise: herpesviruses, virus-cell interactions, vesicular trafficking, signaling



A.E. Gorbalenya

Dept. of Medical Microbiology, Ctr. of Infectious Diseases, Leids Universitair Medisch Centrum (LUMC), Albinusdreef 2, 2333 ZA, Leiden, Netherlands

[Email A.E. Gorbalenya](#)

Area of expertise: Virus Evolution



P.F. Lambert

School of Medicine and Public Health, McArdle Lab. for Cancer Research, University of Wisconsin at Madison, 1400 University Ave, Madison, Wisconsin, 53706, USA

[Email P.F. Lambert](#)

Areas of expertise: Adenoviruses; Polyomaviruses; Parvoviruses; Papillomaviruses; Carcinogenesis by Small DNA Tumor Viruses



S.A. Lommel

Dept. of Plant Pathology, North Carolina State University, 2506 Gardner Hall, Raleigh, North Carolina, NC 27695-7616, USA

[Email S.A. Lommel](#)

Areas of expertise: DNA and RNA Plant Viruses; Viroids



M.H. Malim

Division of Immunology, Infection & Inflammatory Disease, Dept of Infectious Diseases, King's College London, London Bridge, SE1 9RT, London, UK

[Email M.H. Malim](#)

Areas of expertise: HIV; Other Retroviruses



I.J. Molineux

Molecular Genetics & Microbiology, University of Texas, 100 W 24th St, Austin, Texas, TX 78712-1095, USA

[Email I.J. Molineux](#)

Areas of expertise: Bacteriophages; Fungal, yeast, and algal viruses; Virus structure and Assembly



M.B.A. Oldstone

Dept. of Immunology and Microbial Science, The Scripps Research Institute, 10550 N Torrey Pines Rd, La Jolla, California, CA 92037, USA

[Email M.B.A. Oldstone](#)

Areas of expertise: Viral pathogenesis and immunity; Arenaviruses; Measles virus; Unconventional viruses



P. Sarnow

Dept. of Microbiology & Immunology, Stanford University School of Medicine, 299 Campus Dr, Stanford, California, CA 94305, USA

[Email P. Sarnow](#)

Area of expertise: Positive-stranded RNA viruses



B. Sherry

Dept. of Molecular Biomedical Sciences, North Carolina State University, 4700 Hillsborough Street, Raleigh, North Carolina, NC 27606, USA

[Email B. Sherry](#)

Area of expertise: dsRNA viruses; Innate immunity and viral evasion



T.M. Tumpey

Div. of Influenza, Centers for Disease Control and Prevention (CDC), 1600 Clifton Rd. NE., Atlanta, Georgia, GA 30333, USA

[Email T.M. Tumpey](#)

Area of expertise: Orthomyxoviruses



S.P. Whelan

Dept. of Microbiology & Molecular Genetics, Harvard Medical School, 200 Longwood Avenue, Boston, Massachusetts, MA 02115, USA

[Email S.P. Whelan](#)

Areas of expertise: Negative-strand RNA viruses




Highlighted Articles


- [High fidelity simian immunodeficiency virus reverse transcriptase mutants have impaired replication *in vitro* and *in vivo*](#) Original Research Article Open Archive 
Pages 1-10
Sarah B. Lloyd, Marit Lichtfuss, Thakshila H. Amarasena, Sheilajen Alcantara, Robert De Rose, Gilda Tachedjian, Hamid Alinejad-Rokny, Vanessa Venturi, Miles P. Davenport, Wendy R. Winnall, Stephen J. Kent
[▶ Abstract](#) | [▶ Research highlights](#) | [▶ PDF \(1707 K\)](#)


- [Mouse Norovirus infection promotes autophagy induction to facilitate replication but prevents final autophagosome maturation](#) Original Research Article Open Archive 
Pages 130-139
Tanya B. O'Donnell, Jennifer L. Hyde, Justine D. Mintern, Jason M. Mackenzie
[▶ Abstract](#) | [▶ Research highlights](#) | [▶ PDF \(6828 K\)](#)


- [Permissiveness of lepidopteran hosts is linked to differential expression of bracovirus genes](#) Original Research Article Open Archive 
Pages 259-272
Kavita Bitra, Gaelen R. Burke, Michael R. Strand
[▶ Abstract](#) | [▶ Research highlights](#) | [▶ PDF \(769 K\)](#) | [Supplementary content](#)


Regular Articles


- [Characterization of *Enterococcus faecium* bacteriophage IME-EFm5 and its endolysin LysEFm5](#) Original Research Article Open Archive 
Pages 11-20
Pengjuan Gong, Mengjun Cheng, Xinwei Li, Haiyan Jiang, Chuang Yu, Nadire Kahaer, Juecheng Li, Lei Zhang, Feifei Xia, Liyuan Hu, Changjiang Sun, Xin Feng, Liancheng Lei, Wenyu Han, Jingmin Gu
[▶ Abstract](#) | [▶ Research highlights](#) | [▶ PDF \(6041 K\)](#) | [Supplementary content](#)


- [Analysis of HCV-6 isolates among Asian-born immigrants in North America reveals their high genetic diversity and a new subtype](#) Original Research Article Open Archive 
Pages 25-31
Ling Lu, Tao Wu, Lu Xiong, Chunhua Li, Mindie H. Nguyen, Donald G. Murphy
[▶ Abstract](#) | [▶ Research highlights](#) | [▶ PDF \(827 K\)](#)





















- [Role of Jumonji C-domain containing protein 6 \(JMJD6\) in infectivity of foot-and-mouth disease virus](#) Original Research Article Open Archive 
Pages 38-52
Paul Lawrence, Devendra Rai, Joseph S. Conderino, Sabena Uddowla, Elizabeth Rieder
[▶ Abstract](#) | [▶ Research highlights](#) | [▶ PDF \(4746 K\)](#) | [Supplementary content](#)







- [The E glycoprotein plays an essential role in the high pathogenicity of European–Mediterranean IS98 strain of West Nile virus](#) Original Research Article Open Archive 
Pages 53-65
Khaled Alsaleh, Cécile Khou, Marie-Pascale Frenkiel, Sylvie Lecollinet, Ana Vázquez, Eva Ramírez de Arellano, Philippe Després, Nathalie Pardigon
[▶ Abstract](#) | [▶ Research highlights](#) | [▶ PDF \(1720 K\)](#) | [Supplementary content](#)

- [Caveolin- and clathrin-independent entry of BKPyV into primary human proximal tubule epithelial cells](#) Original Research Article Open Archive 
Pages 66-72
Linbo Zhao, Anthony T. Marciano, Courtney R. Rivet, Michael J. Imperiale
[▶ Abstract](#) | [▶ Research highlights](#) | [▶ PDF \(895 K\)](#)

- [Genomic diversity of large-plaque-forming podoviruses infecting the phytopathogen *Ralstonia solanacearum*](#) Original Research Article Open Archive 
Pages 73-81
Takeru Kawasaki, Eriia Narulita, Minaho Matsunami, Hiroki Ishikawa, Mio Shimizu, Makoto Fujie, Anjana Bhunchoth, Namthip Phironrit, Orawan Chatchawankanphanich, Takashi Yamada
[▶ Abstract](#) | [▶ Research highlights](#) | [▶ PDF \(895 K\)](#) | [Supplementary content](#)

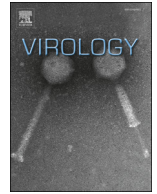
- [Mutational analysis of varicella-zoster virus \(VZV\) immediate early protein \(IE62\) subdomains and their importance in viral replication](#) Original Research Article Open Archive 
Pages 82-91
Mohamed I. Khalil, Xibing Che, Phillip Sung, Marvin H. Sommer, John Hay, Ann M. Arvin
[▶ Abstract](#) | [▶ Research highlights](#) | [▶ PDF \(2244 K\)](#)

- [Triticum mosaic virus exhibits limited population variation yet shows evidence of parallel evolution after replicated serial passage in wheat](#) Original Research Article Open Archive 
 Pages 92-100
 Melissa Bartels, Roy French, Robert A. Graybosch, Satyanarayana Tatineni
[▶ Abstract](#) | [▶ Research highlights](#) |  PDF (1395 K)
- [Development of novel triplex single-step real-time PCR assay for detection of Hepatitis Virus B and C simultaneously](#) Original Research Article Open Archive 
 Pages 101-107
 Shantanu Prakash, Amita Jain, Bhawana Jain
[▶ Abstract](#) | [▶ Research highlights](#) |  PDF (3180 K)
- [Pathogenesis and micro-anatomic characterization of a cell-adapted mutant foot-and-mouth disease virus in cattle: Impact of the Jumonji C-domain containing protein 6 \(JMJD6\) and route of inoculation](#) Original Research Article Open Archive 
 Pages 108-117
 Paul Lawrence, Juan Pacheco, Carolina Stenfeldt, Jonathan Arzt, Devendra K. Rai, Elizabeth Rieder
[▶ Abstract](#) | [▶ Research highlights](#) |  PDF (5728 K)
- [Genetic characterization of an adapted pandemic 2009 H1N1 influenza virus that reveals improved replication rates in human lung epithelial cells](#) Original Research Article Open Access 
 Pages 118-129
 Xenia Wörmann, Markus Lesch, Robert-William Welke, Konstantin Okonechnikov, Mirshat Abdurishid, Christian Sieben, Andreas Geissner, Volker Brinkmann, Markus Kastner, Andreas Kamer, Rong Zhu, Peter Hinterdorfer, Chakkumkal Anish, Peter H. Seeberger, Andreas Herrmann, Thomas F. Meyer, Alexander Karlas
[▶ Abstract](#) | [▶ Graphical abstract](#) | [▶ Research highlights](#) |  PDF (3906 K) | [Supplementary content](#)
- [The Asian-American variant of human papillomavirus type 16 exhibits higher activation of MAPK and PI3K/AKT signaling pathways, transformation, migration and invasion of primary human keratinocytes](#) Original Research Article Open Archive 
 Pages 145-154
 Jimena Hochmann, João S Sobrinho, Luisa L. Villa, Laura Sichero
[▶ Abstract](#) | [▶ Research highlights](#) |  PDF (1222 K) | [Supplementary content](#)
- [Long non-coding RNA GAS5 inhibited hepatitis C virus replication by binding viral NS3 protein](#) Original Research Article Open Archive 
 Pages 155-165
 Xijing Qian, Chen Xu, Ping Zhao, Zhongtian Qi
[▶ Abstract](#) | [▶ Research highlights](#) |  PDF (4376 K) | [Supplementary content](#)
- [Development of tobacco ringspot virus-based vectors for foreign gene expression and virus-induced gene silencing in a variety of plants](#) Original Research Article Open Archive 
 Pages 166-178
 Fumei Zhao, Seungmo Lim, Davaajargal Igori, Ran Hee Yoo, Suk-Yoon Kwon, Jae Sun Moon
[▶ Abstract](#) | [▶ Research highlights](#) |  PDF (3206 K)
- [Viral forensic genomics reveals the relatedness of classic herpes simplex virus strains KOS, KOS63, and KOS79](#) Original Research Article Open Archive 
 Pages 179-186
 Christopher D. Bowen, Daniel W. Renner, Jacob T. Shreve, Yolanda Tafuri, Kimberly M. Payne, Richard D. Dix, Paul R. Kinchington, Derek Gatherer, Moriah L. Szpara
[▶ Abstract](#) | [▶ Research highlights](#) |  PDF (795 K) | [Supplementary content](#)
- [Intravirion cohesion of matrix protein M1 with ribonucleocapsid is a prerequisite of influenza virus infectivity](#) Original Research Article Open Archive 
 Pages 187-196
 O.P. Zhimov, A.A. Manykin, J.S. Rossman, H.D. Klenk
[▶ Abstract](#) | [▶ Research highlights](#) |  PDF (2003 K)
- [A cationic liposome–DNA complexes adjuvant \(JVRS-100\) enhances the immunogenicity and cross-protective efficacy of pre-pandemic influenza A \(H5N1\) vaccine in ferrets](#) Original Research Article Open Archive 
 Pages 197-203
 Feng Liu, Xiangjie Sun, Jeffery Fairman, David B. Lewis, Jacqueline M. Katz, Min Levine, Terrence M. Tumpey, Xiuhua Lu
[▶ Abstract](#) | [▶ Research highlights](#) |  PDF (586 K)

- [HIV-1 nucleocapsid protein localizes efficiently to the nucleus and nucleolus](#) Original Research Article Open Archive 
Pages 204-212
 Kyung Lee Yu, Sun Hee Lee, Eun Soo Lee, Ji Chang You
[▶ Abstract](#) | [▶ Research highlights](#) | [PDF \(9396 K\)](#) | [Supplementary content](#)
- [Hepatitis C virus quasispecies and pseudotype analysis from acute infection to chronicity in HIV-1 co-infected individuals](#) Original Research Article Open Archive 
Pages 213-224
 R. Bridget Ferns, Alexander W. Tarr, Stephane Hue, Richard A. Urbanowicz, C. Patrick McClure, Richard Gilson, Jonathan K. Ball, Eleni Nastouli, Jeremy A. Garson, Deenan Pillay
[▶ Abstract](#) | [▶ Research highlights](#) | [PDF \(1750 K\)](#) | [Supplementary content](#)
- [Comparison of 'HoBi'-like viral populations among persistent infected calves generated under experimental conditions and to inoculum virus](#) Original Research Article Open Archive 
Pages 225-231
 M.N. Weber, F.V. Bauermann, D.O. Bayles, C.W. Canal, J.D. Neill, J.F. Ridpath
[▶ Abstract](#) | [▶ Research highlights](#) | [PDF \(1610 K\)](#) | [Supplementary content](#)
- [Mapping and modeling of a strain-specific epitope in the Norwalk virus capsid inner shell](#) Original Research Article Open Archive 
Pages 232-241
 Gabriel I. Parra, Stanislav V. Sosnovtsev, Eugenio J. Abente, Carlos Sandoval-Jaime, Karin Bok, Michael A. Dolan, Kim Y. Green
[▶ Abstract](#) | [▶ Research highlights](#) | [PDF \(8145 K\)](#) | [Supplementary content](#)
- [Distinct temporal changes in host cell lncRNA expression during the course of an adenovirus infection](#) Original Research Article Open Archive 
Pages 242-250
 Hongxing Zhao, Maoshan Chen, Sara Bergström Lind, Ulf Pettersson
[▶ Abstract](#) | [▶ Research highlights](#) | [PDF \(1967 K\)](#) | [Supplementary content](#)
- [Inability of FMDV replication in equine kidney epithelial cells is independent of integrin \$\alpha\beta 3\$ and \$\alpha\beta 6\$](#) Original Research Article Open Archive 
Pages 251-258
 Yanqin Wang, Qingfu Mao, Huiyun Chang, Yongyan Wu, Shaohui Pan, Yanhe Li, Yong Zhang
[▶ Abstract](#) | [▶ Research highlights](#) | [PDF \(6481 K\)](#)

Brief Communications

- [Local persistence and global dissemination play a significant role in the circulation of influenza B viruses in Leyte Island, Philippines](#) Open Access 
Pages 21-24
 Yuki Furuse, Takashi Odagiri, Raita Tamaki, Taro Kamigaki, Hirono Otomaru, Jamie Opinion, Arlene Santo, Donna Dolina-Lacaba, Edgard Daya, Michiko Okamoto, Mariko Saito-Obata, Marianne Inobaya, Alvin Tan, Veronica Tallo, Socorro Lupisan, Akira Suzuki, Hitoshi Oshitani
[▶ Abstract](#) | [▶ Research highlights](#) | [PDF \(1216 K\)](#) | [Supplementary content](#)
- [A microRNA from infectious spleen and kidney necrosis virus modulates expression of the virus-mock basement membrane component VP08R](#) Open Archive 
Pages 32-37
 Muting Yan, Jianhui He, Weibin Zhu, Jing zhang, Qiong Xia, Shaoping Weng, Jianguo He, Xiaopeng Xu
[▶ Abstract](#) | [▶ Research highlights](#) | [PDF \(3051 K\)](#)
- [Gammaherpesvirus targets peritoneal B-1 B cells for long-term latency](#) Open Archive 
Pages 140-144
 Michaela M. Rekow, Eric J. Darrah, Wadzanai P. Mboko, Philip T. Lange, Vera L. Tarakanova
[▶ Abstract](#) | [▶ Research highlights](#) | [PDF \(442 K\)](#)



Genomic diversity of large-plaque-forming podoviruses infecting the phytopathogen *Ralstonia solanacearum*



Takeru Kawasaki^{a,1}, Eria Narulita^{a,b,1}, Minaho Matsunami^a, Hiroki Ishikawa^a, Mio Shimizu^a, Makoto Fujie^a, Anjana Bhunchoth^c, Namthip Phironrit^c, Orawan Chatchawankanphanich^c, Takashi Yamada^{a,*}

^a Department of Molecular Biotechnology, Graduate School of Advanced Sciences of Matter, Hiroshima University, Higashi-Hiroshima 739-8530, Japan

^b Study Program of Biology Education, University of Jember, Jember 68121, Indonesia

^c National Center for Genetic Engineering and Biotechnology (BIOTEC), National Science and Technology Development Agency (NSTDA), Pathum Thani 12120, Thailand

ARTICLE INFO

Article history:

Received 26 November 2015

Returned to author for revisions

25 January 2016

Accepted 14 February 2016

Keywords:

T7-like phages

φKMV-like phages

Ralstonia solanacearum

Genomic analysis

Host range

ABSTRACT

The genome organization, gene structure, and host range of five podoviruses that infect *Ralstonia solanacearum*, the causative agent of bacterial wilt disease were characterized. The phages fell into two distinctive groups based on the genome position of the RNA polymerase gene (i.e., T7-type and φKMV-type). One-step growth experiments revealed that φRSB2 (a T7-like phage) lysed host cells more efficiently with a shorter infection cycle (ca. 60 min corresponding to half the doubling time of the host) than φKMV-like phages such as φRSB1 (with an infection cycle of ca. 180 min). Co-infection experiments with φRSB1 and φRSB2 showed that φRSB2 always predominated in the phage progeny independent of host strains. Most phages had wide host-ranges and the phage particles usually did not attach to the resistant strains; when occasionally some did, the phage genome was injected into the resistant strain's cytoplasm, as revealed by fluorescence microscopy with SYBR Gold-labeled phage particles.

© 2016 Elsevier Inc. All rights reserved.

1. Introduction

The phytopathogen *Ralstonia solanacearum*, a soil-borne Gram-negative bacterium (Betaproteobacterium), causes bacterial wilt disease in many important crops (Hayward, 1991; Yabuuchi et al., 1995). The unusually wide host-range of this bacterium extends to over 200 species belonging to more than 50 botanical families (Hayward, 2000). *R. solanacearum* strains are a heterogeneous group subdivided into five races on the basis of their host range, six biovars based on their physiological and biochemical characteristics (Hayward, 2000). Race 1 is a poorly defined group with a very wide host range, and is endemic to tropical, subtropical, and warm areas. Strains of race 2 mainly infect bananas, and are found primarily in Southeast Asia and Central America. Race 3 strains are distributed worldwide, and are principally associated with potato. Strains of race 4 infect ginger in areas of Asia and Hawaii, and race 5 strains infect mulberries in China. There is no general correlation between races and biovars. In the recent classification system

based on phylogenetic information (including nucleotide sequences of the 16S–23S ITS, *egl*, *hrpB*, and *mutS*), the strains are sub-grouped into four phylotypes roughly corresponding to their geographic origin. Phylotype I includes strains originating primarily from Asia, phylotype II from America, phylotype III from Africa and surrounding islands in the Indian Ocean, and phylotype IV from Indonesia (Fegan and Prior, 2005; Remenant et al., 2010).

Recently, Yamada et al. (2007) isolated and characterized various types of bacteriophage specifically infecting *R. solanacearum* strains belonging to different races and/or biovars. Among them, φRSB1, which was characterized as a podovirus with a wide host-range, exclusively replicates by a lytic cycle and forms very large plaques (1.0–1.5 cm in diameter) with the cells of *R. solanacearum* strains (Kawasaki et al., 2009). The φRSB1 genome is a linear double-stranded DNA of 43,079 bp with direct terminal repeats of 325 bp. φRSB1 encodes a total of 47 potential same-direction open reading frames (ORFs) arranged in three functional classes known as T7-like podoviruses: one for early functions (Class I), one for DNA metabolism (Class II), and the other for structural proteins (Class III) (Dunn and Studier, 1983). The characteristic features of gene organization in φRSB1 are as follows: (i) the predicted gene for RNA polymerase (RNAP) is not located in the early gene region (Class I) but at the end of the Class II region (similar to that found with φKMV-like phages) (Lavigne et al., 2003); (ii) the predicted

* Correspondence to: Department of Molecular Biotechnology, Graduate School of Advanced Sciences of Matter, Hiroshima University, 1-3-1 Kagamiyama, Higashi-Hiroshima 739-8530, Japan.

E-mail address: tayamad@hiroshima-u.ac.jp (T. Yamada).

¹ These authors contributed equally.

gene for DNA ligase (DNAL) is in front of the RNAP ORF, in contrast to the T7 DNAL gene located downstream of the RNAP gene in Class I (Dunn and Studier, 1983) and to the ϕ KMV DNAL gene located upstream of the gene encoding DNA polymerase (DNAP), and the DNAP gene is located far away from the RNAP gene (Lavigne et al., 2003); and (iii) the core promoter sequences conserved in T3, T7 and SP6 phages are not present in the ϕ RSB1 genes (Kawasaki et al., 2009). For the ϕ RSB1 genomic sequence, podovirus key genes, especially the Class II genes are highly conserved compared with those of various phages including the *Xanthomonas oryzae* phages Xop411 and Xp10 (accession numbers DQ777876 and AY299121, respectively), *Pseudomonas aeruginosa* ϕ KMV (AJ505558), LKD16 and LKA1 (Ceysens et al., 2006), the *Erwinia amylovora* Era103 phage (EF160123), and the *Burkholderia cepacia* BcepF1 phage (AY616033). Thus far, a few ϕ RSB1-like phages have been reported to infect *R. solanacearum* but the molecular biological information is scarce (Tanaka et al., 1990; Toyoda et al., 1991; Ozawa et al., 2001). Recently, extensive surveys of such phages have been performed because they may be useful as tools not only for molecular biological studies of *R. solanacearum* pathogenicity but also for diagnosis and biocontrol of bacterial wilt (Yamada, 2012). Indeed, many podoviruses have been isolated from Japan and Thailand where bacterial wilt occurs very frequently (Bhunchoth et al., 2015).

In this study, we report on the isolation, characterization, and comparative genomics of various podoviruses (distinct from ϕ RSB1) that infect *R. solanacearum* strains.

2. Results

2.1. Morphology and biological properties of large plaque forming phages infecting *R. solanacearum* strains

Bacteriophages ϕ RSB1, ϕ RSB2, ϕ RSB3, ϕ RSJ2 and ϕ RSJ5 were isolated from the soil samples of tomato crop fields and were selected for their ability to form large clear plaques on *R. solanacearum* strains as hosts. Plaques formed on assay plates (CPG)

sometimes extended to 1.0–1.5 cm in diameter (Supplemental Fig. S1). Generally, the bacteriophages had wide host-ranges (except for ϕ RSB3) and infected more than two-thirds of the strains tested, including strains with phylotypes I and IV, races 1, 3 and 4, and biovars 3, 4, and N2 (Table 1). The widest host-range was seen for ϕ RSB1, which infected 19 of the 21 strains tested. ϕ RSB3 infected only five strains of the 21 strains tested. In standard one-step growth assays for ϕ RSB1, *R. solanacearum* host cells (strain MAFF 730138) lysed 140 min after infection with a latent period of 80 min. The cells released approximately 10 plaque forming units (pfu) of new phage particles per cell (burst size) (Supplemental Fig. S2). This burst size was unexpectedly lower than that obtained with strain M4S as the host (100 pfu/cell) although the infection cycle was almost the same (Kawasaki et al., 2009). With such a variation in the burst size (10–100 pfu/cell), the infection cycle was almost the same for the other phages (Bhunchoth et al., 2015), except for ϕ RSB2. In the case of ϕ RSB2, phage infection occurred more rapidly with MAFF 730138 as the host, where an infection cycle of 60 min with a latent period of 40 min (eclipse of 20 min) give a burst size of ca. 30 pfu/cell (Fig. 1). For comparison, the one-step growth of ϕ RSB1 with strain MAFF 730138 as the host is given as a supplemental material (Fig. S2). The characteristic infection cycles are discussed below. Electron microscopic observation of negatively stained phage particles from ϕ RSB1, ϕ RSB2, ϕ RSB3, ϕ RSJ2 and ϕ RSJ5 revealed short-tailed icosahedral structures resembling those of T7-like phages of the *Podoviridae* family, with a head diameter of approximately 60 nm and a stubby tail with a length of 8–10 nm. The morphologies and dimensions of the particles from all these phages were very similar to each other (data not shown) and to podoviruses isolated in Thailand, where bacterial wilt occurred frequently (Bhunchoth et al., 2015).

3. Genome sequencing and ORF identification of *Ralstonia* podoviruses

The genomic DNA isolated from particles of each phage always migrated as a single band of approximately 40–50 kbp in size on

Table 1
Comparison of host range of the phages.

Phage host strain	ϕ RSB1 (KMV-like) EOP adsorption		ϕ RSB2 (T7-like) EOP adsorption		ϕ RSB3 (KMV-like) EOP adsorption	
C319	+(< 1)	38.2 ± 5.2	+(100)	95.3 ± 3.2	–	2.2 ± 1.0
M4S	+(1000)	45.2 ± 1.3	–	91 ± 1.2	+(1000)	77.5 ± 4.2
Ps29	+(100)	81.2 ± 3.5	–	5.3 ± 2.6	+(10)	67.5 ± 1.0
Ps65	+(< 1)	39.5 ± 6.5	+(100)	8.5 ± 7.2	–	0.9 ± 1.5
Ps72	+(< 1)	45.3 ± 2.8	+(1000)	79.1 ± 1.4	–	41.4 ± 3.0
Ps74	+(42)	23.7 ± 2.5	+(400)	40.1 ± 4.8	+(70)	67.5 ± 1.0
RS1002	+(2)	70.9 ± 1.6	–	8.5 ± 5.9	–	63.0 ± 4.7
MAFF106603	+(5)	12.3 ± 5.2	+(1000)	54.6 ± 12.2	–	29.2 ± 2.9
MAFF106611	+(2)	38.8 ± 6.4	–	38.8 ± 6.5	–	54.4 ± 6.5
MAFF211270	–	33.3 ± 5.8	+(3)	66.9 ± 5.2	–	5.1 ± 4.5
MAFF211271	+(270)	47.1 ± 9.7	+(400)	40 ± 16.5	–	0.0 ± 0.0
MAFF211272	+(4250)	40.4 ± 4.3	+(4000)	37.8 ± 3.9	–	8.0 ± 6.9
MAFF211514	+(< 1)	35.4 ± 12.1	–	26.1 ± 8.5	+(210)	13.2 ± 2.4
MAFF301485	+(< 1)	57.9 ± 7.2	+(150)	72.3 ± 6.3	–	34.3 ± 6.1
MAFF301556	+(< 1)	82.3 ± 0.6	–	2.6 ± 2.1	–	52.7 ± 5.7
MAFF301558	+(120)	10.4 ± 3.1	+(500)	77.4 ± 4.6	–	18.5 ± 8.0
MAFF327032	–	24.2 ± 13.8	+(10)	79.3 ± 4.0	–	23.9 ± 7.7
MAFF730103	+(5)	32.1 ± 3.1	–	16.8 ± 3.7	–	76.0 ± 11.4
MAFF730135	+(< 1)	76.4 ± 7.6	–	5.3 ± 3.7	–	76.0 ± 2.3
MAFF730138	+(120)	14.1 ± 5.0	+(300)	42.8 ± 11.8	+(60)	17.3 ± 5.6
MAFF730139	+(8)	71.4 ± 0.6	+(3400)	32.8 ± 10.3	–	3.3 ± 5.8
Total	19		13		5	

+, sensitive; –, resistant. Numbers in parentheses are relative efficiency of plating (EOP, original host is shown as 1000). Numbers on the right side are adsorption rates of the phage (%). Standard deviations were calculated from three independent experiments. For host ranges of ϕ RSJ2 and ϕ RSJ5, see Bhunchoth et al. (2015).

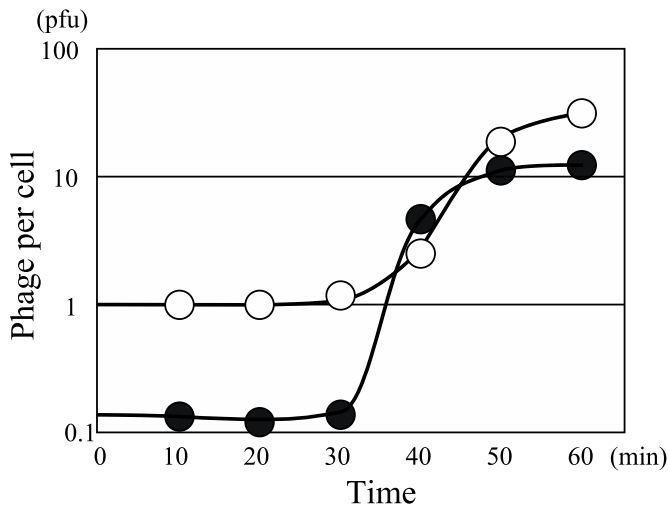


Fig. 1. One-step growth curve of ϕ RSB2 with strain MAFF 730138 as the host. Phage (grown with the same host) was added at a moi of 0.1 and allowed to adsorb for 5 min. The ϕ RSB2-infected culture was added with 1 mM EGTA at 30 min post infection. The titers were determined by the standard method with (closed circles) or without (open circles) chloroform treatment.

Table 2
Genomic comparison of *R. solanacearum* phages.

Phages	G+C (%)	Genome size (bp)	Terminal repeats (bp)	ORFs	Accession no.
ϕ RSB1	61.7	43,079	325	47	AB451219
ϕ RSB2	61.7	40,411	214	50	AB597179
ϕ RSB3	61.0	44,578	324	50	AB854109
ϕ RSJ 2	60.9	44,684	324	43	AB920995
ϕ RSJ 5	60.7	44,067	322	42	AB983711

pulsed-field gels (data not shown) indicating it was a linear double-stranded (ds) DNA molecule. Because no oligomers were formed after heat treatment, cohesive ends are absent. The nucleotide sequence of each phage genome was determined by shotgun sequencing of DNA purified from the phage particles, as described in Section 5. In each case, sequences were assembled into a circular contig, suggesting the presence of long terminal repeats. By direct sequencing of genomic DNA with outward-directed primers located outside the possible terminal repeat region, the precise sequence of the repeat was determined. The final genomic sequences of ϕ RSB2, ϕ RSB3, ϕ RSJ2 and ϕ RSJ5 were as follows: ϕ RSB2, 40,411 bp with 214-bp repeats; ϕ RSB3, 44,578 bp with 324-bp repeats; ϕ RSJ2, 44,684 bp with 324-bp repeats; ϕ RSJ5, 44,067 bp with 322-bp repeats. These sizes are comparable with that of ϕ RSB1 (Kawasaki et al., 2009) (Table 2). The G+C contents of the phage genomes were 60.7–61.7%, which is significantly lower than the values of 67.04% and 66.86% obtained for the large and small replicons of the *R. solanacearum* GM11000 genome, respectively (Salanoubat et al., 2002).

When the entire genomic nucleotide sequences of these phages were compared with each other by dot-plot alignments, it was found that the sequence homology and collinearity varied significantly between the phages (Supplemental Fig. S3). Extended sequence homology was seen between ϕ RSJ2 and ϕ RSJ5 (Supplemental Fig. S4) and sequence collinearity degraded from ϕ RSB1– ϕ RSJ2 to ϕ RSJ2– ϕ RSB3. ϕ RSB2 shared only local and limited homology with the other phages (i.e., the RNA polymerase-encoding region and the 3'-terminal region) see below.

Potential ORFs consisting of more than about 50 codons that start with ATG or GTG were identified within each phage genome. The presence of a Shine–Dalgarno ribosome-binding sequence preceding the initiation codon was taken into account for the ORF predictions. To assign possible functions to the ORFs, database searches were conducted using BLAST, BLASTX, and BLASTP programs. Accordingly, 50, 50, 43, and 42 potential ORFs oriented in

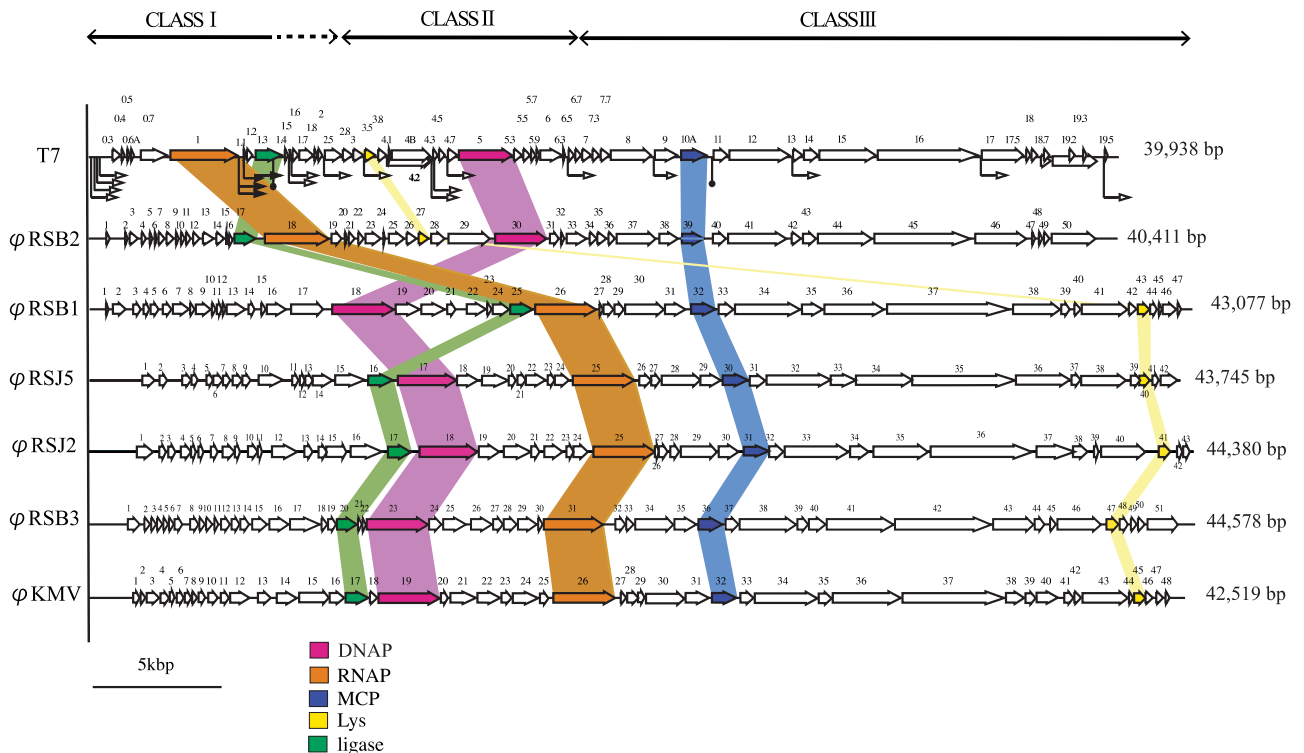


Fig. 2. Comparison of the five *Ralstonia* podovirus gene maps with those of *Escherichia coli* T7 and *Pseudomonas aeruginosa* ϕ KMV. The regions corresponding to T7 Class I, II, and III functional modules are shown. The genes corresponding to DNA polymerase (DNAP), RNA polymerase (RNAP), major capsid protein (MCP), lysozyme (Lys), and DNA ligase (ligase) are shown in different colors.

the same direction were assigned to the ϕ RSB2, ϕ RSB3, ϕ RSJ2 and ϕ RSJ5 genomes, respectively (Table 2 and Fig. 2). In many cases, the stop codon of an ORF overlapped with (or was very close to) the initiation codon of the following ORF in the phage genomes.

3.1. Comparative genome organization analysis of *Ralstonia podoviruses*

In a previous study on ϕ RSB1 genes, 13 (*orf1-orf13*), 13 (*orf14-orf26*), and 21 (*orf27-orf47*) of them were assigned to Class I, II and III, respectively, based on their promoter/terminator positions and proteomic analysis (Kawasaki et al., 2009). Comparisons with the ϕ RSB1 gene organization showed that the borders of the Class I–Class II, and Class II–Class III, were *orf13-orf14* and *orf25-orf26* for ϕ RSJ5, *orf14-orf15* and *orf25-orf26* for ϕ RSJ2, and *orf15-orf16* and *orf31-orf32* for ϕ RSB3, respectively. Most ϕ RSJ2 and ϕ RSJ5 Class I genes shared high nucleotide sequence similarity with the Class I genes of ϕ RSB3, while ϕ RSJ2 and ϕ RSJ5 Class II genes shared sequence similarity with the Class II genes of ϕ RSB1, thereby supporting the way in which the gene sorting has been conducted and suggesting that module exchanges have occurred among the phages.

For ϕ RSB2, the Class I–Class II border was unclear because of the presence of many unknown genes in this region. After *orf21*, there was a putative terminator structure and *orf23* showed homology to the DNMP kinase, so the border was tentatively set as *orf21-orf22* in ϕ RSB2. The Class II–Class III border was determined to be *orf34-orf35* by comparing it with the organization of ϕ RSB1.

There are two distinct subgroups in T7-like podoviruses: the T7 subgroup (Hardies et al., 2003; Molineux, 2006) and the ϕ KMV subgroup (Lavigne et al., 2003; Ceysens et al., 2006). The most obvious difference in the genome organization between these two subgroups is the position of the viral RNAP gene; in T7, it is located in the Class I region whereas in ϕ KMV, it is within the Class II region of the genome. Using the genomic organizations of T7 and ϕ KMV as references, the gene arrangements of the five phages were compared with each other. As shown in Fig. 2, the RNAP gene was obviously located within the Class I region in the ϕ RSB2 genome. In this respect, ϕ RSB2 belongs to the T7 subgroup. For the other four phages (ϕ RSB1, ϕ RSB3, ϕ RSJ2, and ϕ RSJ5), the RNAP gene was located within Class II, downstream of the DNAP gene as shown in Fig. 2, indicating that all of these phages are the ϕ KMV subgroup. However, in comparison with the ϕ KMV gene arrangement, the position of the DNA ligase gene was changed from a position upstream of the DNAP gene to a position in front of the RNAP gene in ϕ RSB1. This gene order (DNAL–RNAP) was conserved in the Class I region of ϕ RSB2. The other obvious difference in the gene arrangement was the location of *lys*; in the ϕ KMV subgroup phages, *lys* was located on the right-hand end region of the genome, while it was between the RNAP gene and the DNAP gene in the ϕ RSB2 genome.

3.2. Putative promoter and terminator sequences

A typical prokaryotic promoter sequence resembling that of *Escherichia coli* σ^{70} was found to be repeated several times in a left, 1000-bp region lacking ORFs in ϕ RSB2, ϕ RSB3, ϕ RSJ2 and ϕ RSJ5, as seen in ϕ RSB1 (Kawasaki et al., 2009). Searches for the core promoter-like sequences conserved in T3, T7, and SP6 phages in the intergenic regions of ϕ RSB1, ϕ RSB3, ϕ RSJ2 and ϕ RSJ5 (the ϕ KMV subgroup phages) did not find any significant ones except for ϕ RSB2 (the T7 subgroup phage), where a total of 14 sequences with significant homology to the T3-promoter were detected. These T3-like promoter sequences were found mainly in the Class II and III regions after *map* (ORF18) in the ϕ RSB2 genome (Supplemental Fig. S5). The consensus sequence of the ϕ RSB2 PNAP

promoters was 5'-NAT TAA CCC ACA CTR YAG GAR RRS, a sequence 65% identical to that of the T3 phage (5'-AAT TAA CCC TCA CTA AAG GGA GA). These results indicate that ϕ RSB2 depends on its RNAP for major genes expressed in the intermediate and late stages of the infection cycle.

Although a set of sequence elements consisting of a GC-rich stretch, TTGT, and TCTGG motifs preceding an AG-rich Shine–Dalgarno sequence were previously suggested to correspond to ϕ RSB1 promoter sites (Kawasaki et al., 2009), such sequences were not always conserved in other phages (ϕ RSB3, ϕ RSJ2, and ϕ RSJ5). These motifs did not correspond to the nick consensus sites (Kulakov et al., 2009) and no nicks (Wang et al., 2005) were detected in these phages. Further detailed searches for promoter sequences for these phages were not conducted in this study.

3.3. Early genes and DNA replication genes

The genes for early functions encoded in the Class I region of these *Ralstonia* phages showed a diverse organization and sequences (Fig. 2). When the RNAP amino acid sequences of related phages were aligned and analyzed by ClustalW, three groups of *Ralstonia* phages were evident: a cluster of ϕ RSB1, ϕ RSJ2 and ϕ RSJ5, a T7-cluster including T3 and ϕ RSB2, and a ϕ KMV-cluster including *Pseudomonas* phages and ϕ RSB3 (Supplemental Fig. S6A). The close relationship in the RNAP sequence between T7 and ϕ RSB2 was consistent with the location of the ϕ RSB2 RNAP gene in the Class I region.

In all of these *Ralstonia* phages, the genes in the Class II cluster for DNA metabolism were arranged generally in the same order as that of T7 DNA; they included genes for DNA primase, DNA helicase, DNA polymerase, and DNA endonuclease VII. One exception was the gene for DNA ligase (DNAL), where *orf25* encoding ϕ RSB1 DNAL was in front of the RNAP ORF, whereas T7 DNAL was encoded downstream of the RNAP gene at the end of the Class I cluster (Dunn and Studier, 1983). In the case of ϕ RSB2, the DNAL gene was immediately upstream of the RNAP gene. As in the *Pseudomonas* phage ϕ KMV, the DNAL gene was located upstream of the DNAP gene in the Class II gene cluster of ϕ RSB3, ϕ RSJ2 and ϕ RSJ5 (Fig. 2). When DNAP and DNAL amino acid sequences were aligned and analyzed by ClustalW for related phages, the DNAP sequences showed almost the same relationships found for the RNAP sequences; namely, three clusters of *Ralstonia* phages (Supplemental Fig. S6B). However, the DNAL sequences suggested very different phylogenetic relationships among these phages, with ϕ RSB3 forming a close relationship with ϕ RSJ2, ϕ RSJ5 and ϕ RSB1 in the *Xanthomonas* phage cluster (Supplemental Fig. S6C).

3.4. Phage structural proteins and lysis genes

ϕ RSB1 structural genes (Kawasaki et al., 2009) in the Class III region were highly conserved in other *Ralstonia* phages (Fig. 2). The amino acid sequences of the putative major capsid protein (MCP) of these phages when compared by ClustalW with those of several T7-like phages, showed the three-group pattern similar to that found with the RNAP and DNAP sequences (Supplemental Fig. S6D). In many T7-like phages, genes for host lysis (lysozyme and a holin) are placed between the genes for endonuclease and DNA primase in the Class II cluster. However, ϕ RSB2 ORF27, which corresponds to lysozyme (LYS), is encoded in the middle of the Class II region. In other phages (ϕ RSB1, ϕ RSB3, ϕ RSJ2, and ϕ RSJ5), the gene for LYS is encoded downstream of the structural gene cluster in the Class III region (Fig. 2). Three phylogenetic LYS sequence groups in the *Ralstonia* phages were revealed by ClustalW analysis as shown in Supplemental Fig. S6E.

3.5. Host selection in *Ralstonia podoviruses*

As shown in Table 1, the *Ralstonia* phages displayed relatively wide host-ranges for strains belonging to races 1, 3, and 4 and phylotypes I and IV, except for ϕ RSB3, which infected five among 21 of the strains tested. There seemed to be no close relationships between phage sensitivity and taxonomical position of these strains. To visualize the actual interactions between these phages and the host strains, the adsorption efficiency of ϕ RSB1, ϕ RSB2, and ϕ RSB3 was determined for each host strain representative of the three clusters. The data shown in Table 1 reveals the following complex patterns for the interactions: (i) all sensitive strains were adsorbed with their corresponding phages, (ii) some resistant strains were not efficiently adsorbed with phages (exemplified by ϕ RSB2 and MAFF 211271), and (iii) some resistant strains were efficiently adsorbed by phages (exemplified by ϕ RSB2 and M4S). These results indicate that the adsorption efficiency does not always determine the infectivity of a phage to *R. solanacearum* strains. Consequently, this raises the question as to what happened in the cells after phage adsorption.

To examine the fate of the adsorbed phages, SYBR Gold-stained phage particles were added to the cells of each strain and fluorescence microscopy was performed. When M4S cells were added to SYBR Gold-stained ϕ RSB1, the phage particles attached to the cells and the cells became stained with the dye 30 min post infection (p.i.) as shown in Fig. 3A. This was most likely caused by injection of SYBR Gold-stained ϕ RSB1 DNA into the host cells. In contrast, SYBR Gold-labeled ϕ RSB3 particles did not attach to MAFF 211271 cells (Fig. 3B). This was also the case for C319, Ps65, MAFF 211270, MAFF 211272, and MAFF 730139 host cells.

Nevertheless, SYBR Gold-labeled ϕ RSB3 particles attached efficiently to cells of the resistant strain (MAFF730135) but no DNA injection was observed (Fig. 3D). The same results with SYBR Gold-labeled ϕ RSB3 particles were obtained for MAFF 106603, MAFF 106611 and MAFF 730103 cells. However, in some cases, DNA injection was observed even in the resistant cells (Fig. 3C) when MAFF 211270 cells were added to SYBR Gold-labeled ϕ RSB1 particles and the DNA injected was retained in the cell for a while. The same situation was observed for SYBR Gold-labeled ϕ RSB2 and M4S.

3.6. Effects of phage adsorption on the bacterial growth

To see effects of phage adsorption on host cells, the bacterial growth was monitored in specific combinations of phage and host strains. Phage was added to exponentially growing cells (at $OD_{600}=0.3$) at multiplicity of infection (moi) 0.1, 1.0, or 10, and the cell growth was measured at OD_{600} . In the case of strain MAFF 730135 added with ϕ RSB3, where phage attachment occurred without DNA injection (Fig. 3D), no significant difference in the successive growth was observed between phage added cells (even at moi 10) and control cells (without phage addition) (Fig. 4A). This was exactly the same as the results observed for strain MAFF 211271 added with ϕ RSB3 (no attachment occurred, Fig. 3B) (data not shown). Meanwhile, the growth curve of MAFF 211270 after addition of ϕ RSB1 showed significant decline in the growth, depending on moi values (Fig. 4B). When cell viability was tested by direct plating on CPG plates, 30 min after addition of ϕ RSB1, approximately 4% of MAFF 211270 cells added with phage at moi 1.0 and 12% of cells at moi 10 could not form colonies, respectively

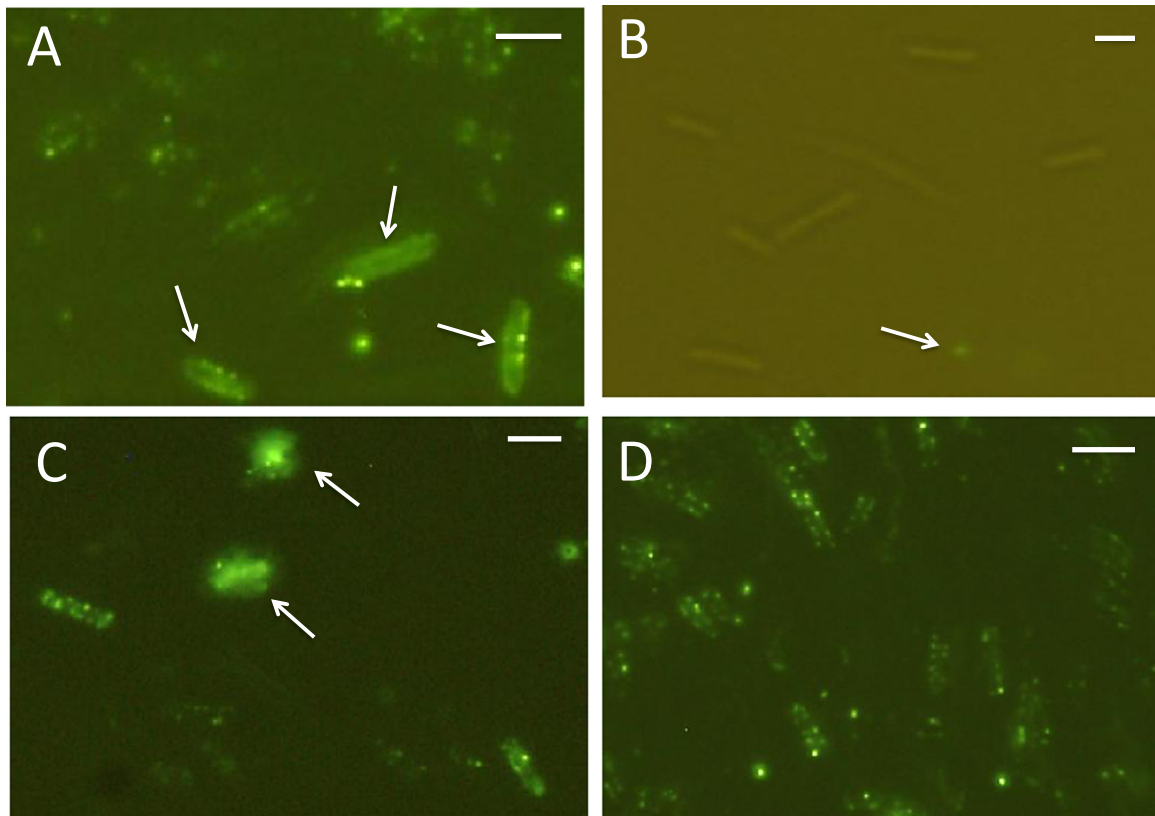


Fig. 3. Attachment of SYBR Gold-labeled phage particles to bacterial cells and cell staining by possible injection of phage DNA. (A) SYBR Gold-stained ϕ RSB1 particles (tiny spots) are attached to the M4S cells (sensitive strain). The cells were stained with the dye at 30 min post infection (p.i.) as shown by arrows. (B) SYBR Gold-labeled ϕ RSB3 particles did not attach to MAFF211271 cells (resistant strain). To visualize the bacterial cells, the bright and dark fields were combined. Arrow indicates a phage particle. (C) SYBR Gold-labeled ϕ RSB1 particles attached to MAFF211270 (resistant strain) and injected genomic DNA into the cells (arrows). (D) SYBR Gold-labeled ϕ RSB3 particles efficiently attached to MAFF730135 cells (resistant strain) but no DNA injection was observed. The particles: pfu was different for different strains. Bar = 1.0 μ m.

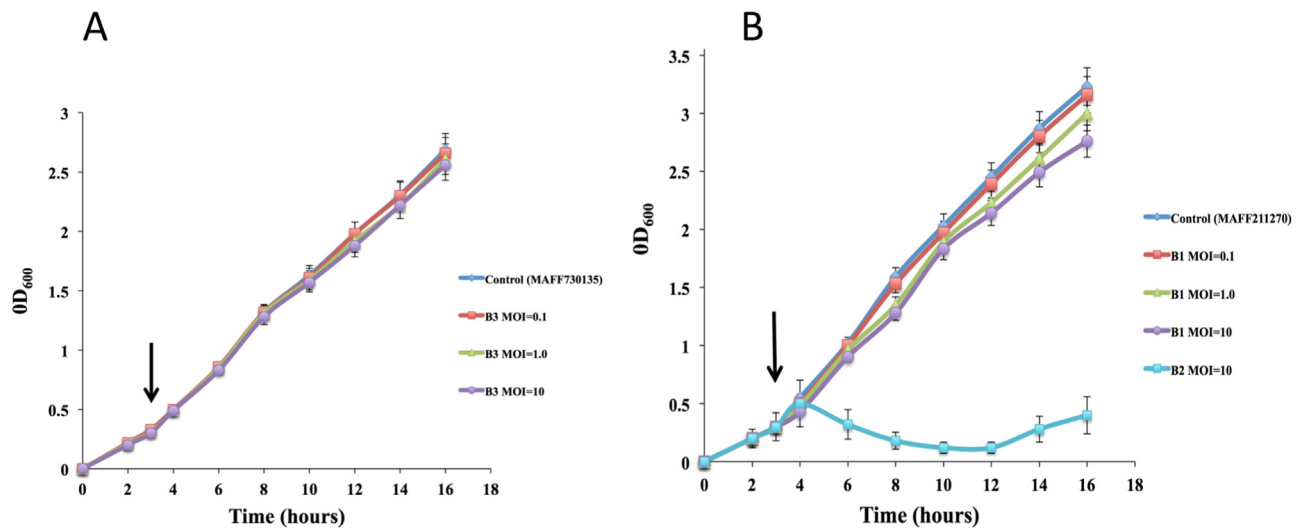


Fig. 4. Time course of bacterial growth after infection with bacteriophages. Cells of *R. solanacearum* ($OD_{600}=0.3$, corresponding to $\sim 10^8$ cfu/ml; vertical arrow) were added with phages at moi=0.1, 1.0, or 10. (A) Cells of strain MAFF 730135 were added with ϕ RSB3. (B) Cells of strain MAFF 211270 were added with ϕ RSB1. For a control, susceptible phage ϕ RSB2 was added at moi 10 in the same way. Data from three independent experiments are shown with standard deviations.

(Supplemental Table S2). These results suggested that ϕ RSB1 attachment and DNA injection to MAFF 211270 (Fig. 3C) caused some inhibitory effects on the cell growth (partially killing effects).

3.7. Infectivity compared between ϕ RSB1 (ϕ KMV-type) and ϕ RSB2 (T7-type) in the same strain

As described above, ϕ RSB1 (ϕ KMV-like) had a wider host range but a relatively longer infection cycle and ϕ RSB2 (T7-like) showed a limited host range but a short infection cycle. Both phages share common hosts as shown in Table 1, so that infectivity could be compared between the two phages in the same host strains. When ϕ RSB1 and ϕ RSB2 were co-infected to the same strain as a host, ϕ RSB2 always predominated in the phage progeny independent of host strains. For example, MAFF 211272 giving similar titers for each phage (Table 1), the percentage of ϕ RSB1 in the phage progeny [ϕ RSB1/(ϕ RSB1+ ϕ RSB2)] infected at moi=3 was $2.5 \pm 0.68\%$ (calculated from four experiments). Superinfection by ϕ RSB2 of ϕ RSB1-infected cells resulted in production of only ϕ RSB2 in the lysate unless superinfection was delayed until close to the end of the latent period. These results indicated that in *R. solanacearum* strains, ϕ RSB2 (T7-like) with a shorter infection cycle (Fig. 1) easily win the competition over ϕ RSB1 (ϕ KMV-like) with a longer infection cycle under laboratory conditions. The possibility of recombination between the two phages was examined by plaque hybridization with specific probes of each genomic DNA. No plaque was detected that hybridized to both probes in the phage progenies after co-infection (data not shown).

4. Discussion

Podoviruses that infect *R. solanacearum* strains are widespread in the environment (Bhunchoth et al., 2015). In most cases, they form large clear plaques with different hosts. In this study, five phage isolates from Japan and Thailand, which showed very different genomic DNA-*Hinc*II restriction patterns, were compared with each other. Based on the genomic organization and sequence similarity of the main podovirus genes, they generally grouped into the following two types: T7-like phages (ϕ RSB2-type) and ϕ KMV-like phages, with the latter divided further into two sub-groups (ϕ RSB1-type and ϕ RSB3-type). ϕ RSB2 encodes its RNAP gene in the Class I region of the genome (Fig. 2) and has many

phage T3-like transcriptional promoter sequence elements in the Class II and III regions (Supplemental Fig. S5). This genomic organization fits well with the temporal transcriptional regulation known for T7-like phages (McAllister and Wu, 1978), where transcription of phage early genes (Class I) relies on host RNAP and late transcription (for Class II and III genes) in the phage encoding RNAP. In contrast, the RNAP gene in ϕ RSB1-type and ϕ RSB3-type phages is distal to the Class II region in the genome (Fig. 2) and no conserved promoter sequence for phage RNAP was obvious. The genome location of the phage RNAP downstream of the DNA replication genes, and the absence of conserved T7-like phage promoter sequences, implies a higher dependency on the host RNAP for transcription of early phage genes, and perhaps even for other genes (Fig. 2 and Supplemental Fig. S5). In comparison with the infection pattern observed for ϕ KMV-type phages such as ϕ RSB1 (Kawasaki et al., 2009) and ϕ RSJ2 (Bhunchoth et al., 2015), ϕ RSB2 (T7-type phage) lysed the host cells very quickly. As shown in Fig. 1, the ϕ RSB2 infection cycle took 60 min with eclipse and latent periods of 20 min and 40 min, respectively. This infection cycle is considerably shorter than that of ϕ KMV-type phages (90–180 min for one cycle with a latent period of 60–90 min). In the case of ϕ RSB2, the gene for RNAP is located within the Class I module and there are 14 phage-specific promoters distributed throughout Class I to III modules (Supplemental Fig. S5), suggesting that an authentic T7-like gene expression strategy operates in this phage. With the same strain (MAFF 730138) as the host, ϕ RSB1 (ϕ KMV-like phage) and ϕ RSB2 (T7-like phage) provided a good opportunity to experimentally compare the efficiency of gene expression by the different types of phage-encoded RNA polymerase. In the co-infection experiments where ϕ RSB1 and ϕ RSB2 were added to the same strain as a host, ϕ RSB2 always predominated in the phage progeny independent of host strains. This result can be simply interpreted as the faster's win in the infection race. No recombination between the two phages was detected. Contrasting to this infective superiority of ϕ RSB2 (T7-like phage) under laboratory conditions, we observed an obvious predominant distribution of ϕ KMV-like phages in natural environments (Bhunchoth et al., 2015). When podoviruses isolated from different soil samples (more than 15) were characterized by genomic Southern blot hybridization with ϕ RSB1 RNAP-DNA and ϕ RSB1 ORF24-DNA (Class II gene) as probes, all but one (ϕ RSB2) showed the ϕ RSB1-type (ϕ KMV-like) gene organization (data not shown). There should be some factors affecting the infectivity of

these phages, for example, stability of phage particles in the natural environment.

Here, our one-step growth experiments also revealed unexpectedly low burst sizes for the phages with some host strains (e.g., ~10 pfu/cell for ϕ RSB1 with MAFF 730138 as the host). This burst size is significantly lower than that of coliphage T7 (120 pfu/cell). In the one-step growth experiments, this may have been caused by frequent adsorption of phage particles (filled with DNA) to the cell debris immediately after release, as was frequently observed by electron microscopy (data not shown). Phage recovery was increased by vortexing or addition of 1 mM EGTA to the ϕ RSB1-infected host culture (the burst size increased from 10 pfu/cell to 15–20 pfu/cell) (Supplemental Fig. S2). Alternatively, somewhat unsynchronized lysis (due to poor adsorption) of host cells might also result in many immature phage particles in the lytic cycle. Moreover, mechanisms of abortive infection may work in host cells to resist some types of phage. For ϕ RSB1 infection of the MAFF 730138 strain, under conditions where more than 50% of the host cells adsorbed phage particles, a burst size of ~10 pfu per cell only was obtained. This suggests the possibility that most cells with phage particles attached died without producing phage progenies, and only a few were able to do so. This mechanism may also explain the sensitivity and host range of these phages. Indeed, we observed cell growth inhibition in MAFF 211270 cells after ϕ RSB1 attachment and injection of its DNA into the cells (Fig. 4B).

As can be seen in Table 1, the five *Ralstonia* podoviruses have different host ranges. Three different conditions in the phage-resistant cells were revealed by fluorescence microscopy of cells infected with SYBR-gold labeled phages: (i) low adsorption of phages to the cell, (ii) positive adsorption but no injection of phage DNA into the cells, and (iii) positive adsorption and injection of DNA into the cells. The former two conditions may be explained by the insufficient interaction between phage receptors on the cells and host binding proteins on the virion. The last condition invokes several possibilities including the following: phage resistance systems acquired by bacterial cells (Labrie et al., 2010) include restriction-modification systems (Tock and Dryden, 2005), abortive infection (Chopin et al., 2005), Argonaute-based interference (Swarts et al., 2014), and clustered regularly interspaced short palindromic repeats (CRISPR) and associated protein (Cas) adaptive immune system (Barrangou and Marraffini, 2014; Van der Oost et al., 2014). The toxin-antitoxin systems may also work in cells attached by phages (Anantharaman and Aravind, 2003). Recently, BREX, a novel system for bacteriophage exclusion in bacteria was reported as an innate immunity mechanism against virulent and temperate phages (Goldfarb et al., 2015). The phage-resistant strains displaying a type iii response (Fig. 4) may drive an unknown abortive infection mechanism. It is important to understand such a mechanism if there is to be efficient utilization of bacteriophages for the biocontrol of plant diseases.

5. Materials and methods

5.1. Bacterial strains and phages

The *R. solanacearum* strains used in this study are listed in Supplemental Table S1. The host species and taxonomic features of these strains are also included in the Table. Bacterial cells were cultured in CPG medium containing 0.1% casamino acids, 1% peptone and 0.5% glucose (Horita and Tsuchiya, 2002) at 28 °C with shaking at 200–300 rpm. Bacteriophage ϕ RSB1 was the same line as that used in previous work (Kawasaki et al., 2009). Phages ϕ RSB2 and ϕ RSB3 were isolated and purified from soil samples collected in August, 2008 from tomato crop fields in Higashi-Hiroshima, Japan in the same way as described previously (Yamada et

al., 2007). Phages ϕ RSJ2 and ϕ RSJ5 were isolated from soil samples collected in tomato fields in Chiang Mai, Thailand, 2013 (Bhunchoth et al., 2015). Phages were routinely propagated in strains M4S (for ϕ RSB1 and ϕ RSB3) or MAFF106603 (for ϕ RSB2, ϕ RSJ2 and ϕ RSJ5) as the hosts. At 16–24 h of culture, the bacterial cells grown in CPG medium were diluted 100-fold with 100 ml of fresh CPG medium in a 500-ml flask. To collect sufficient phage particles, 1.0 L of bacterial culture was grown. When the cultures reached a 0.2 unit of OD₆₀₀, the phage was added at a multiplicity of infection (moi) of 0.001–1.0. After further growth for 9–18 h, the cell debris was removed by centrifugation in the R12A2 rotor of a Hitachi himac CR21E centrifuge (Hitachi Koki Co. Ltd., Tokyo, Japan) at 8000 × g for 15 min at 4 °C. The supernatant was passed through a 0.2- μ m membrane filter and the phage particles were precipitated by centrifugation with a P28S rotor in a Hitachi CP100 β centrifuge at 40,000 × g for 1 h at 4 °C and then dissolved in SM buffer (50 mM Tris-HCl at pH 7.5, 100 mM NaCl, 10 mM MgSO₄, and 0.01% gelatine). Purified phages were stored at 4 °C until use. For the morphological studies, phage particles purified by CsCl-gradient ultracentrifugation (with a P28S rotor in a Hitachi CP100 β ultracentrifuge) were stained with Na-phosphotungstate before observation in a Hitachi H600A electron microscope, according to the method of Dykstra (1993). λ phage particles were used as an internal standard marker for size determination. *E. coli* XL10 Gold and pBluescript II SK(+) were obtained from Stratagene (La Jolla, CA).

5.2. DNA manipulation and sequencing

Standard molecular biological techniques for DNA isolation, digestion with restriction enzymes and other nucleases, and construction of recombinant DNA molecules were followed according to the methods of Sambrook and Russell (2001). Phage DNA was isolated from purified phage particles by phenol extraction. For genome size determination, the purified phage particles were embedded in 0.7% low-melting-point agarose (InCert agarose, FMC Corp, Philadelphia, PA) and after treatment with proteinase K (1 mg/ml, Merck Ltd., Tokyo, Japan) and 1% Sarkosyl, were subjected to pulsed-field gel electrophoresis using CHEF MAPPER electrophoresis apparatus (Bio-Rad Lab., Hercules, CA) according to Higashiyama and Yamada (1991). Shotgun sequencing was performed at Hokkaido System Science Co., Ltd. (Sapporo, Japan) using a Roche GS Junior Sequence System. The draft assembly of the sequences obtained was achieved using GS De Novo Assembler, GS Reference Mapper v2.6 (Roche). The sequences analyzed corresponded to 30, 40, 174, and 236 times the final contig sizes of ϕ RSB2 (40,197 bp), ϕ RSB3 (44,254 bp), ϕ RSJ2 (44,360 bp), and ϕ RSJ5 (43,745 bp), respectively. Potential ORFs larger than 150 bp (50 codons) were identified using Glimmer (Delcher et al., 1999) and GeneMark (<http://exon.gatech.edu/GeneMark/>). Homology searches were performed using BLAST/RPS-BLAST (Altschul et al., 1997) against the UniProt sequence database (UniProt Consortium, 2007) and the NCBI/CDD database (Wheeler et al., 2007), using an *E*-value lower than 10⁻⁴ as a cutoff for notable similarity. Multiple sequence alignments were generated using the DNASIS program (version 3.6; Hitachi Software Engineering, Co., Ltd., Tokyo, Japan). For phylogenetic analysis of RNA polymerase (RNAP), DNA polymerase (DNAP), DNA ligase (DNAL), tail fiber (TF) and major capsid (MCP) proteins, the unrooted dendrograms were constructed with the Treeview tool using the maximum likelihood method based on the complete protein sequence alignment of the corresponding proteins from other phages using ClustalX. The terminal repeat sequences of each phage DNA were determined according to the method used for ϕ RSB1 (Kawasaki et al., 2009).

5.3. Host range and efficiency of plating

Host ranges of purified phages were generally determined by the serial dilution spot test method with a panel of *R. solanacearum* strains as hosts. Soft agar overlays (0.75% in CPG) containing 100 μ l bacterial cells ($\sim 10^8$ cfu/ml) as an indicator host were allowed to solidify, spotted with 10- μ l drops of serially diluted phage preparations, and assayed after incubation at 28 °C for 3–5 days. Filtrates producing either plaques or cleared zones were serially diluted in SM-buffer and assayed by using the overlay method, where 100 μ l of each dilution was mixed directly with the host suspension in tempered soft agar before overlaying. Efficiency of plating (EOP) was determined by calculating the ratio of the phage plaque titer obtained with a heterologous (non-propagating) host to that obtained with a homologous (propagating) host.

5.4. Single-step growth experiments and phage adsorption assays

Single-step growth experiments were performed as described previously (Carlson, 1994; Kawasaki et al., 2009) with some modifications. *R. solanacearum* MAFF 730138 cells (0.5 U of OD₆₀₀) were harvested by centrifugation and resuspended in fresh CPG (ca. 3×10^7 CFU/ml). Phage (grown with MAFF 730138 as the host) was added at a moi of 0.1 and allowed to adsorb for 5 min at room temperature. After centrifugation and resuspension in CPG, the cells were incubated at 28 °C. The phage-infected culture was added with 1 mM EGTA at 30 min post infection. Samples were taken at 10-min intervals up to 3 h with or without chloroform treatment, and the titers were determined by the double-layered agar plate method (Kawasaki et al., 2009). The phage adsorption assay involved adding phage to a 450- μ l culture of *R. solanacearum* (0.5 U of OD₆₀₀ in CPG; ~ 50 μ l, diluted with CPG) at a moi of 0.01 in an Eppendorf tube followed by incubation at 28 °C for 30 min. After centrifugation (6000 $\times g$, 5 min), 200 μ l of the supernatant was filtrated through a membrane filter (0.45- μ m pore size), then subjected to the plaque assay. *E. coli* XL10 Gold grown in LB was used as a control. Experiments were repeated three times and the data were statistically treated. Adsorption ratio = $100 \times (1 - X/X_c)$, where X and X_c were the number of plaques that appeared on the assay plates with a tested strain and a control, respectively. The host strains used for propagation and plaque assays were M4S for ϕ RSB1 and ϕ RSB3 and MAFF106603 for ϕ RSB2, respectively.

5.5. Coinfection of ϕ RSB1 and ϕ RSB2 in different host strains

To compare growth efficiency between ϕ RSB1 (ϕ KMV-like) and ϕ RSB2 (T7-like) in the same strain, coinfection experiments were conducted. Each of ϕ RSB1 and ϕ RSB2 was propagated in strain MAFF 730138 as the common host and their respective titers were determined by plaque forming assay for test strains (heterologous strains) as hosts, including MAFF 211272 (the titer was different depending on the heterologous strains). For phage infection, each host strain was grown in 6 ml of CPG at 28 °C to 0.1 U of OD₆₀₀ and added with a mixture (1 ml) of ϕ RSB1 and ϕ RSB2 at a moi of 3 (for each phage). After adsorption for 15 min, the cells were spun down by centrifugation at 4000 $\times g$ for 5 min at room temperature, resuspended in CPG, and incubated at 28 °C. Samples were taken and filtrated through a membrane filter (0.45- μ m pore size) at 3 h after infection. Individual plaques (900 plaques or more) formed from these samples on CPG plates with the same host strain were tested for infectivity to strain MAFF 327032 and M4S as the host to identify whether ϕ RSB1 or ϕ RSB2.

5.6. Staining of bacterial cells by SYBR Gold-labeled phages

Phage labeling and phage-treated bacterial cell observation were performed according to Mosier-Boss et al. (2003). To 100 ml of phage lysate, 10 μ l of $10^4 \times$ SYBR Gold (Molecular Probes, Inc., Eugene, OR, USA) in DMSO was added. After 10 min, the labeled phage particles were precipitated by centrifugation with a P28S rotor in a Hitachi XII100 β centrifuge at 40,000 $\times g$ for 1 h at 4 °C. Three washes with $1 \times$ PBS were performed to ensure excess SYBR Gold was removed. A 1-ml sample of an overnight culture of *R. solanacearum* was mixed with 4-ml CPG and allowed to grow until an OD₆₀₀ of 0.5 was reached. A 10- μ l sample of the bacterial culture was added to 10 μ l of SYBR Gold-labeled phage and the solution was incubated for 10–60 min. The particles: pfu was different for different strains.

As a control, a culture of *E. coli* JM109 was treated in the same way. The bacterial cells were observed under a fluorescence microscope with filter sets (Olympus BX-2 fluorescence microscope; Olympus, Tokyo, Japan). Microscopic images were recorded with a CCD camera (Keyence VB-6010; Osaka, Japan).

5.7. Nucleotide sequence accession numbers

The sequence data for genomic DNA from ϕ RSB2, ϕ RSB3, ϕ RSJ2, and ϕ RSJ5 have been deposited in the DDBJ database under the accession numbers AB597179, AB854109, AB920995 and AB983711, respectively.

Conflict of interest

The authors have no conflict of interest to declare.

Acknowledgments

This study was supported by the Strategic Japanese-Thai Research Cooperative Program on Biotechnology (JST/BIOTEC-SICP). The authors would like to thank Taiki Yasuda, Takaya Sonomoto and Abdelmonim Ali Ahmad for assisting with the one-step growth experiments, the mixed infection assays and the SYBR-gold staining experiments, respectively.

Appendix A. Supplementary material

Supplementary data associated with this article can be found in the online version at <http://dx.doi.org/10.1016/j.virol.2016.02.011>.

References

- Altschul, S.F., Madden, T.L., Schaffer, A.A., Zhang, Z., Miller, W., Lipman, D.J., 1997. Gapped BLAST and PSI-BLAST: a new generation of protein database search programs. *Nucleic Acids Res.* 25, 3389–3402.
- Anantharaman, V., Aravind, L., 2003. New connections in the prokaryotic toxin-antitoxin network: relationship with the eukaryotic nonsense-mediated RNA decay system. *Genome Biol.* 4, R81.
- Barrangou, R., Marraffini, L.A., 2014. CRISPR-Cas systems: prokaryotes upgrade to adaptive immunity. *Mol. Cell* 54, 234–244.
- Bhunchoth, A., Phironrit, N., Leksomboon, C., Chatchawankanphanich, O., Kotera, K., Narulita, E., Kawasaki, T., Fujie, M., Yamada, T., 2015. Isolation of *Ralstonia solanacearum*-infecting bacteriophages from tomato fields in Chiang Mai, Thailand, and their experimental use as biocontrol agents. *J. Appl. Microbiol.* 118, 1023–1033.
- Carlson, K., 1994. Single-step growth. In: Karam, J., Drake, J.W., Kreuzer, K.N., Mosig, G., Hall, D.H., Eiserlig, F.A., Black, L.W., Spicer, E.K., Kutter, E., Carlson, K., Miller, E.S. (Eds.), *Molecular Biology of Bacteriophage T4*. ASM press, Washington, D. C, pp. 434–437.

- Ceyssens, P.-J., Lavigne, R., Mattheus, W., Chibeu, A., Hertveldt, K., Mast, J., Robben, J., Volckaert, G., 2006. Genomic analysis of *Pseudomonas aeruginosa* phages LKD16 and LKA1: establishment of the ϕ KMV subgroup within the T7 subgroup. *J. Bacteriol.* 188, 6924–6931.
- Chopin, M.C., Chopin, A., Bidnenko, E., 2005. Phage abortive infection in lactococci: variants on a theme. *Curr. Opin. Microbiol.* 8, 473–479.
- Delcher, A.L., Harmon, D., Kasif, S., White, O., Salzberg, S.L., 1999. Improved microbial gene identification with GLIMMER. *Nucleic Acids Res.* 27, 4636–4641.
- Dunn, J.J., Studier, F.W., 1983. Complete nucleotide sequence of bacteriophage T7DNA and the locations of T7 genetic elements. *J. Mol. Biol.* 166, 477–535.
- Dykstra, M.J., 1993. *A Manual of Applied Technique for Biological Electron Microscopy*. Plenum Press, New York.
- Fegan, M., Prior, P., 2005. How complex is the “*Ralstonia solanacearum* species complex”? In: Allen, C., Prior, P., Hayward, A.C. (Eds.), *Bacterial Wilt Disease and the Ralstonia solanacearum Species Complex*. APS Press, St. Paul, pp. 449–461.
- Goldfarb, T., Sberro, H., Weinstock, W., Cohen, O., Doron, S., Charpak, A., Afik, S., Ofir, G., Sorek, R., 2015. BREX, a phage resistance system widespread in microbial genomes. *EMBO J.* 34, 169–183.
- Hardies, S.C., Comeau, A.M., Serwer, P., Suttle, C.A., 2003. The complete sequence of marine bacteriophage VpV262 infecting *Vibrio parahaemolyticus* indicates that an ancestral component of a T7 viral supergroup is widespread in the marine environment. *Virology* 310, 359–371.
- Hayward, A.C., 1991. Biology and epidemiology of bacterial wilt caused by *Pseudomonas solanacearum*. *Annu. Rev. Phytopathol.* 29, 65–87.
- Hayward, A.C., 2000. *Ralstonia solanacearum*. In: Lederberg, J. (Ed.), *Encyclopedia of Microbiology*, 4. Academic Press, San Diego, C. A., pp. 32–42.
- Higashiyama, T., Yamada, T., 1991. Electrophoretic karyotyping and chromosomal gene mapping of *Chlorella*. *Nucleic Acids Res.* 19, 6191–6195.
- Horita, M., Tsuchiya, K., 2002. Causal agent of bacterial wilt disease *Ralstonia solanacearum*. In: National Institute of Agricultural Sciences (Ed.), *MAFF Microorganism Genetic Resources Manual No. 12*. National Institute of Agricultural Sciences, Tsukuba, Japan, pp. 5–8.
- Kawasaki, T., Shimizu, M., Satsuma, H., Fujiwara, A., Fujie, M., Usami, S., Yamada, T., 2009. Genomic characterization of *Ralstonia solanacearum* phage ϕ RSB1, a T7-like wide-host-range phage. *J. Bacteriol.* 191, 422–427.
- Kulakov, L.A., Ksenzenko, V.N., Shlyapnikov, M.G., Kochentkov, V.V., Del Casale, A., Allen, C.C., Larkin, M.J., Ceyssens, P.L., Lavigne, R., 2009. Genomes of “ ϕ iKMV-like viruses” of *Pseudomonas aeruginosa* contain localized single-strand interruptions. *Virology* 391, 1–4.
- Labrie, S.J., Samson, J.E., Moineau, S., 2010. Bacteriophage resistance mechanisms. *Nat. Rev. Microbiol.* 8, 317–327.
- Lavigne, Rob, Burkal'tseva, Maria V, Robben, Johan, Sykilinda, Nina N, Kurochkina, Lidia P, Grymonprez, Barbara, Jonckx, Bart, Krylov, Victor N, Mesyanzhinov, Vadim V, Volckaert, Guido, 2003. The genome of bacteriophage ϕ KMV, a T7-like virus infecting *Pseudomonas aeruginosa*. *Virology* 312 (1), 49–59. [http://dx.doi.org/10.1016/S0042-6822\(03\)00123-5](http://dx.doi.org/10.1016/S0042-6822(03)00123-5).
- McAllister, W.T., Wu, H.-L., 1978. Regulation of transcription of the late genes of bacteriophage T7. *Proc. Natl. Acad. Sci. USA* 75, 804–808.
- Molineux, I.J., 2006. The T7 group. In: Calendar, R. (Ed.), *The Bacteriophages*. Oxford University Press, New York, pp. 277–301.
- Mosier-Boss, P.A., Lieberman, S.H., Andrews, J.M., Rohwer, F.L., Wegley, L.E., Breitbart, M., 2003. Use of fluorescently labeled phage in the detection and identification of bacterial species. *Appl. Spectrosc.* 57, 1138–1144.
- Ozawa, H., Tanaka, H., Ichinose, Y., Shiraiishi, T., Yamada, T., 2001. Bacteriophage P4282, a parasite of *Ralstonia solanacearum*, encodes a bacteriolytic protein important for lytic infection of its host. *Mol. Genet. Genomics* 265, 95–101.
- Remenant, B., Coupat-Goutaland, B., Guidot, A., Cellier, G., Wicker, E., Allen, C., Fegan, M., Pruvost, O., Elbaz, M., Calteau, A., Salvignol, G., Mornico, D., Mangenot, S., Barbe, V., Medigue, C., Prior, P., 2010. Genomes of three tomato pathogens within the *Ralstonia solanacearum* species complex reveal significant evolutionary divergence. *BMC Genomics* 11, 379.
- Salanoubat, M., Genin, S., Artiguenave, F., Gouzy, J., Mangenot, S., Ariat, M., Billault, A., Brottier, P., Camus, J.C., Cattolico, L., Chandler, M., Choisene, N., Claudel-Renard, S., Cunnac, N., Gaspin, C., Lavie, M., Molsan, A., Robert, C., Saurin, W., Schlex, T., Siguier, P., Thebault, P., Whalen, M., Wincker, P., Levy, M., Weissenbach, J., Boucher, C.A., 2002. Genome sequence of the plant pathogen *Ralstonia solanacearum*. *Nature* 415, 497–502.
- Sambrook, J., Russell, D.W., 2001. *Molecular Cloning: A Laboratory Manual*, 3rd ed. Cold Spring Harbor Laboratory Press, Cold Spring Harbor, New York N.Y.
- Swarts, D.C., Makarova, K., Wang, Y., Nakanishi, K., Ketting, R.F., Koonin, E.V., Patel, D.J., van der Oost, J., 2014. The evolutionary journey of the Argonature proteins. *Nat. Struct. Mol. Biol.* 21, 743–753.
- Tanaka, H., Negishi, H., Maeda, H., 1990. Control of tobacco bacterial wilt by an avirulent strain of *Pseudomonas solanacearum* M4S and bacteriophage. *Ann. Phytopathol. Soc. Jpn* 56, 243–246.
- Tock, M.R., Dryden, D.T., 2005. The biology of restriction and anti-restriction. *Curr. Opin. Microbiol.* 8, 466–472.
- Toyoda, H., Kakutani, K., Ikeda, S., Goto, S., Tanaka, H., Ouchi, S., 1991. Characterization of deoxyribonucleic acid of virulent bacteriophage and its infectivity to host bacterium *Pseudomonas solanacearum*. *J. Phytopathol.* 131, 11–21.
- UniProt Consortium, 2007. The universal protein resource (UniProt). *Nucleic Acids Res.* 35, D193–D197.
- Van der Oost, J., Westra, E.R., Jackson, R.N., Wiedenheft, B., 2014. Unravelling the structural and mechanistic basis of CRISPR-Cas systems. *Nat. Rev. Microbiol.* 12, 479–492.
- Wang, J., Jiang, Y., Vincent, M., Sun, Y., Yu, H., Wang, J., Bao, Q., Kong, H., Hu, S., 2005. Complete genome sequence of bacteriophage of bacteriophage T5. *Virology* 332, 45–65.
- Wheeler, D.L., Barrett, T., Benson, D.A., Bryant, S.H., Canese, K., Chetvrn, V., Church, D.M., DiCuccio, M., Edgar, E., Federhen, S., Geer, L.Y., Kapustin, Y., Khovayko, O., Landsman, D., Lipman, D.J., Madden, T.L., Maglott, D.R., Ostell, J., Miller, V., Pruitt, K.D., Schuler, G.D., Sequeira, E., Sherry, S.T., Sirotkin, K., Souvorov, A., Starchenko, G., Tatusov, R.L., Tatusova, T.A., Wagner, L., Yaschenko, E., 2007. Database resources of the national center for biotechnology information. *Nucleic Acids Res.* 35, D5–D12.
- Yabuuchi, E., Kosako, V., Yano, I., Hotta, H., Nishiuchi, Y., 1995. Transfer of two *Burkholderia* and an *Alcaligenes* species to *Ralstonia* gen. nov.: proposal of *Ralstonia pickettii* (Ralston, Palleroni and Doudoroff 1973) comb. nov., *Ralstonia solanacearum* (Smith 1896) comb. nov. and *Ralstonia eutropha* (Davis 1969) comb. nov. *Microbiol. Immunol.* 39, 897–904.
- Yamada, T., 2012. Bacteriophages of *Ralstonia solanacearum*: their diversity and utilization as biocontrol agents in agriculture. In: Kurtboke, I. (Ed.), *Bacteriophages*. InTech-Open Access Publisher, Rijeka, Croatia, pp. 113–139.
- Yamada, T., Kawasaki, T., Nagata, S., Fujiwara, A., Usami, S., Fujie, M., 2007. New bacteriophages that infect the phytopathogen *Ralstonia solanacearum*. *Microbiology* 153, 2630–2639.